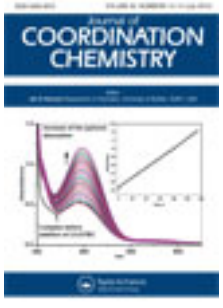

Journal of Coordination Chemistry
Publication details, including instructions for authors and subscription information:
http://www.tandfonline.com/loi/gcoo20

Unsaturation in binuclear iron trifluorophosphine carbonyl derivatives: comparison with binary iron carbonyls

Shida Gong [a], Chaoyang Wang [a], Qian-Shu Li [a], Yaoming Xie [b] & R. Bruce King [a b]

[a] MOE Key Laboratory of Theoretical Chemistry of Environment, Center for Computational Quantum Chemistry, South China Normal University, Guangzhou 510631, P.R. China

[b] Department of Chemistry and Center for Computational Chemistry, University of Georgia, Athens, GA 30602, USA

Accepted author version posted online: 29 May 2012.Published online: 08 Jun 2012.

To cite this article: Shida Gong, Chaoyang Wang, Qian-Shu Li, Yaoming Xie & R. Bruce King (2012) Unsaturation in binuclear iron trifluorophosphine carbonyl derivatives: comparison with binary iron carbonyls, Journal of Coordination Chemistry, 65:14, 2459-2477, DOI: 10.1080/00958972.2012.696108

To link to this article: http://dx.doi.org/10.1080/00958972.2012.696108

Journal of Coordination Chemistry
Vol. 65, No. 14, 20 July 2012, 2459–2477

Unsaturation in binuclear iron trifluorophosphine carbonyl derivatives: comparison with binary iron carbonyls

SHIDA GONG†, CHAOYANG WANG†, QIAN-SHU LI*†, YAOMING XIE‡ and R. BRUCE KING*†‡

†MOE Key Laboratory of Theoretical Chemistry of Environment, Center for Computational Quantum Chemistry, South China Normal University, Guangzhou 510631, P.R. China
‡Department of Chemistry and Center for Computational Chemistry, University of Georgia, Athens, GA 30602, USA

(*Received 8 March 2012; in final form 26 April 2012*)

Bridging PF_3 groups are obviously very unfavorable as indicated by their absence in $Fe_2(CO)_n(PF_3)_2$ ($n = 7, 6, 5, 4$) complexes optimized by density functional theory even though many such structures have one or more bridging CO groups. Except for some $Fe_2(CO)_7(PF_3)_2$ structures, the two terminal PF_3 groups are bonded to different irons. Structures of the saturated $Fe_2(CO)_7(PF_3)_2$ having one, two, and three bridging or semibridging CO groups have similar energies suggesting a fluxional system. The lowest energy structures for the unsaturated $Fe_2(CO)_n(PF_3)_2$ ($n = 6, 5, 4$) derivatives are triplet spin-state structures. However, higher energy singlet $Fe_2(CO)_n(PF_3)_2$ ($n = 6, 5, 4$) structures are found having formal iron–iron multiple bonds and various combinations of bridging and terminal CO groups leading to the favored 18-electron configurations for iron. Most singlet $Fe_2(CO)_n(PF_3)_2$ ($n = 6, 5, 4$) structures are analogous to those of the previous studied $Fe_2(CO)_{n+2}$ structures.

Keywords: Iron; Trifluorophosphine; Density functional theory; Metal carbonyls

1. Introduction

Binuclear iron carbonyl derivatives have been studied experimentally and theoretically for more than a century. Thus $Fe_2(CO)_9$ was first synthesized in 1905 [1] and shown to have three bridging carbonyl groups in the early days of X-ray crystallography [2]. An accurate determination of the geometrical parameters by X-ray was subsequently carried out by Cotton *et al*. in 1974 [3]. The unsaturated $Fe_2(CO)_8$ was first observed spectroscopically as a transient species by Poliakoff and Turner [4] in 1971 and subsequently characterized by Fletcher *et al*. [5] in 1986, and by Fedrigo *et al*. [6] in 1996. Fletcher *et al*. [5] identified two different $Fe_2(CO)_8$ isomers. The dominant isomer appeared to have a doubly bridged structure. The second $Fe_2(CO)_8$ isomer was suggested to have an unbridged structure with an infrared ν(CO) spectrum consistent with D_{2h} geometry. The geometries and energies of the complete series of binuclear

*Corresponding author. Email: qsli@scnu.edu.cn; rbking@chem.uga.edu

ISSN 0095-8972 print/ISSN 1029-0389 online © 2012 Taylor & Francis
http://dx.doi.org/10.1080/00958972.2012.696108

iron carbonyl derivatives, $Fe_2(CO)_n$ ($n = 9, 8, 7, 6$), have been studied by theoretical methods [7, 8].

Trifluorophosphine in metal trifluorophosphine complexes is recognized as a strong acceptor like carbon monoxide, undoubtedly because of the electron-withdrawing properties of the three highly electronegative fluorines [9–18]. Thus PF_3, like CO, stabilizes low formal oxidation states so that many binary (i.e., homoleptic) zerovalent $M(PF_3)_n$ derivatives are relatively stable toward air oxidation. The first of these zerovalent derivatives, $Ni(PF_3)_4$, was synthesized by Irvine and Wilkinson in 1951 using the reaction of $Ni(PCl_3)_4$ with excess PF_3 at ambient pressure [19, 20]. Kruck and coworkers [21] showed that use of high PF_3 pressures allowed the synthesis of additional binary zerovalent metal trifluorophosphine complexes including $Cr(PF_3)_6$, $Fe(PF_3)_5$, and $Pt(PF_3)_4$ [22–24]. Some of these binary metal trifluorophosphine complexes are found to be more stable than the corresponding homoleptic metal carbonyls. Good examples of binary metal trifluorophosphine complexes without stable currently known binary metal carbonyl counterparts include $M_2(PF_3)_8$ (M = Rh and Ir) [25] and $Pt(PF_3)_4$ [13, 14, 26].

These observations of the higher stability of metal trifluorophosphine complexes relative to corresponding metal carbonyls suggested that metal trifluorophosphine chemistry might develop into a more extensive area of inorganic chemistry than even metal carbonyl chemistry. However, as metal trifluorophosphine chemistry continued to evolve, it became apparent that whereas metal trifluorophosphine complexes with terminal PF_3 groups were generally more stable than their carbonyl counterparts, metal trifluorophosphine complexes with bridging PF_3 groups analogous to well-known metal carbonyls having bridging carbonyl groups such as $Fe_2(CO)_9$ [$=Fe_2(CO)_6(\mu\text{-}CO)_3$] and $Co_2(CO)_8$ [$=Co_2(CO)_6(\mu\text{-}CO)_2$] remained unknown. The cobalt derivative $Co_2(PF_3)_8$, analogous in stoichiometry to $Co_2(CO)_8$, has been reported [27] but has not yet been characterized structurally. Theoretical studies [28] predict an unbridged $(F_3P)_4Co$–$Co(PF_3)_4$ structure for $Co_2(PF_3)_8$. The iron derivative $Fe_2(PF_3)_9$ analogous to $Fe_2(CO)_9$ remains unknown. The lowest energy $Fe_2(PF_3)_9$ structure is predicted to be a $(F_3P)_4Fe \leftarrow PF_2Fe(F)(PF_3)_4$ structure in which a P–F bond in one of the PF_3 ligands has split to form a terminal fluoride and a bridging difluorophosphine (PF_2) [29].

The iron trifluorophosphine complex $Fe(PF_3)_5$ is among the binary metal trifluorophosphine complexes that were synthesized by Kruck and co-workers [30, 31] using elevated pressures of PF_3. In addition, the series of ternary iron carbonyl trifluorophosphine complexes $Fe(PF_3)_n(CO)_{5-n}$ ($n = 1, 2, 3, 4, 5$) were synthesized by Clark in 1964 [32]. Photolysis of these ternary iron carbonyl trifluorophosphine complexes provides possible routes to trifluorophosphine substitution products of $Fe_2(CO)_9$ of the type $Fe_2(PF_3)_n(CO)_{9-n}$. Further photolysis of $Fe_2(PF_3)_n(CO)_{9-n}$ potentially can lead to unsaturated ternary trifluorophosphine iron carbonyls of the type $Fe_2(PF_3)_n(CO)_{m-n}$ ($m = 8, 7, 6$).

This article explores possible structures for binuclear trifluorophosphine iron carbonyls of the general type $Fe_2(PF_3)_2(CO)_n$ ($n = 7, 6, 5, 4$) using density functional theory (DFT). The 18-electron rule predicts a formal Fe–Fe bond order of $8 - n$ assuming that all CO and PF_3 groups are two-electron donors. Binuclear derivatives of this type can be possibly synthesized by photolysis of $Fe(PF_3)(CO)_4$. We were particularly interested in seeing whether unusual behavior of the trifluorophosphine ligand could be observed in the highly unsaturated systems. In any case, comparison of the preferred structures of the binuclear ternary compounds $Fe_2(PF_3)_2(CO)_n$

($n = 7, 6, 5, 4$) with those of the corresponding binary iron carbonyls $Fe_2(CO)_{n+2}$ is of interest.

2. Theoretical methods

Electron correlation effects were considered using DFT methods, which have evolved as a practical and effective computational tool, especially for organometallic compounds [33–39]. Two DFT methods were used in this study. The popular B3LYP method combines the three-parameter Becke functional (B3) [40] with the Lee–Yang–Parr (LYP) generalized gradient correlation functional [41]. The BP86 method combines Becke's 1988 exchange functional (B) [42] with Perdew's 1986 gradient corrected correlation functional (P86) [43]. The BP86 method has been found to be somewhat more reliable than the B3LYP method for the organometallic systems considered in this article, especially for the prediction of vibrational frequencies [44–46]. However, Reiher and coworkers have found that B3LYP always favors the high-spin state and BP86 favors the low-spin state for a series of the Fe(II)-S complexes [47]. This is also true for the molecules studied in this article so that these two DFT methods may predict global minima in different spin states. For this reason, Reiher and coworkers have proposed a new parametrization for the B3LYP functional, named B3LYP*, which provides electronic state orderings in agreement with experiment. In addition, these same authors test this B3LYP* functional with the G2 test set and obtain satisfactory results [48]. In this study, we also adopted the B3LYP* method to give more reliable energy differences between the singlet and triplet structures. Thus, in order to have a conclusive energy ordering, we mainly discuss the B3LYP* geometries and energies in the text. The corresponding results from the B3LYP and BP86 methods are shown in the "Supplementary material."

Basis sets have been chosen to provide continuity with a body of existing research on organometallic compounds. Fortunately, DFT methods are less basis set sensitive than higher level methods, such as coupled cluster theory. In this work, all computations were performed using double-ζ plus polarization (DZP) basis sets. The DZP basis sets used for carbon, oxygen, and fluorine add one set of pure spherical harmonic d functions with orbital exponents $\alpha_d(C) = 0.75$, $\alpha_d(O) = 0.85$, and $\alpha_d(F) = 1.0$ to the standard Huzinaga–Dunning contracted DZ sets [49, 50], designated (9s5p1d/4s2p1d). For phosphorus, an additional set of pure spherical harmonic d functions with orbital exponents $\alpha_d(P) = 0.60$, designated (12s8p1d/6s4p1d), was used [51]. The loosely contracted DZP basis set for iron is the Wachters [52] primitive set augmented by two sets of p functions and one set of d functions, contracted following Hood, Pitzer, and Schaefer [53], and designated (14s11p6d/10s8p3d). For $Fe_2(CO)_7(PF_3)_2$, $Fe_2(CO)_6(PF_3)_2$, $Fe_2(CO)_5(PF_3)_2$, and $Fe_2(CO)_4(PF_3)_2$ there are 444, 414, 384, and 354 contracted Gaussian functions, respectively.

The geometries of all structures were fully optimized using the DZP B3LYP, DZP BP86, and DZP B3LYP* methods. Vibrational frequencies were determined by evaluating analytically the second derivatives of the energy with respect to the nuclear coordinates. The corresponding infrared intensities were also evaluated analytically. All of the computations were carried out with the Gaussian 03 program [54], exercising the fine grid option (75 radial shells, 302 angular points) for evaluating integrals

numerically, while the finer grid (120, 974) was only used to double check the small imaginary vibrational frequencies.

In the search for minima using all currently implemented DFT methods, low magnitude imaginary vibrational frequencies are suspect because of significant limitations in the numerical integration procedures used in the DFT computations. Thus all imaginary vibrational frequencies with a magnitude less than $100i\,cm^{-1}$ are considered questionable and are given less weight in the analysis [55]. Therefore, we do not always follow such low imaginary vibrational frequencies. All harmonic vibrational frequencies ν(CO) and $\nu(PF_3)$ and the corresponding infrared intensities are listed in "Supplementary material."

3. Results

3.1. $Fe_2(CO)_7(PF_3)_2$

Five singlet structures, from **7-1S** to **7-5S**, were found having energies within 7 kcal mol^{-1} (figure 1 and table S1 in the Supplementary material). Structure **7-1S** is predicted to have the lowest energy, while structures **7-2S** and **7-3S** are nearly degenerate with **7-1S**. This small energy difference suggests fluxionality for the $Fe_2(CO)_7(PF_3)_2$ system. The higher energy $Fe_2(CO)_7(PF_3)_2$ structures **7-4S** and **7-5S** lie 5.7 and 7.0 kcal mol^{-1}, respectively, above **7-1S**. All of these $Fe_2(CO)_7(PF_3)_2$ structures have only real vibrational frequencies, indicating that they are genuine minima. The triplet $Fe_2(CO)_7(PF_3)_2$ structures lie at least 20 kcal mol^{-1} above **7-1S** and thus are not reported in this article.

The $Fe_2(CO)_7(PF_3)_2$ structures **7-1S** (C_2), **7-2S** (C_1), **7-4S** (C_1), and **7-5S** (C_2) all have a single CO bridge, but structure **7-3S** (C_{2v}) has three CO bridges. Structure **7-1S** also has a highly unsymmetrical semibridging CO group with a short Fe–C distance of 1.829 Å and a long Fe–C distance of 2.575 Å. None of the $Fe_2(CO)_7(PF_3)_2$ structures have bridging PF_3 groups. In **7-2S** and **7-4S**, the two PF_3 groups are linked to the same Fe, while in the other three structures, the two PF_3 are linked to different Fe atoms. The Fe–Fe bond distances predicted by the B3LYP* method are ~2.5 Å for the triply bridged structure **7-3S** and 2.65 to 2.77 Å for the singly bridged structures **7-1S**, **7-2S**, **7-4S**, and **7-5S**. The Fe–Fe bonds in all of these $Fe_2(CO)_7(PF_3)_2$ structures are considered to be formal single bonds, thereby giving each iron in each structure the favored 18-electron configuration. The shortening of a metal–metal bond of a given order, such as the Fe–Fe single bonds in the $Fe_2(CO)_7(PF_3)_2$ structures, is a commonly observed feature of the structures of binuclear metal carbonyl complexes as the number of bridging carbonyls is increased.

The bridging CO groups in these $Fe_2(CO)_7(PF_3)_2$ structures are indicated by their ν(CO) frequencies (table S21). In such compounds the bridging ν(CO) region is around 1840 cm^{-1}, which is 50–150 cm^{-1} lower than the terminal ν(CO) frequencies [5]. Compared with the $\nu(\mu$-CO) frequencies of 1870, 1870, and 1895 cm^{-1} for $Fe_2(CO)_9$ at the same level [7], the similar triply bridged $Fe_2(\mu\text{-}CO)_3(CO)_3(PF_3)_2$ structure **7-3S** has slightly lower $\nu(\mu$-CO) frequencies of 1847, 1859, and 1887 cm^{-1}. This suggests that the $d\pi \rightarrow p\pi^*$ backbonding to the bridging CO groups in the ternary derivative $Fe_2(\mu\text{-}CO)_3(CO)_3(PF_3)_2$ is stronger than that in the binary derivative $Fe_2(\mu\text{-}CO)_3(CO)_6$.

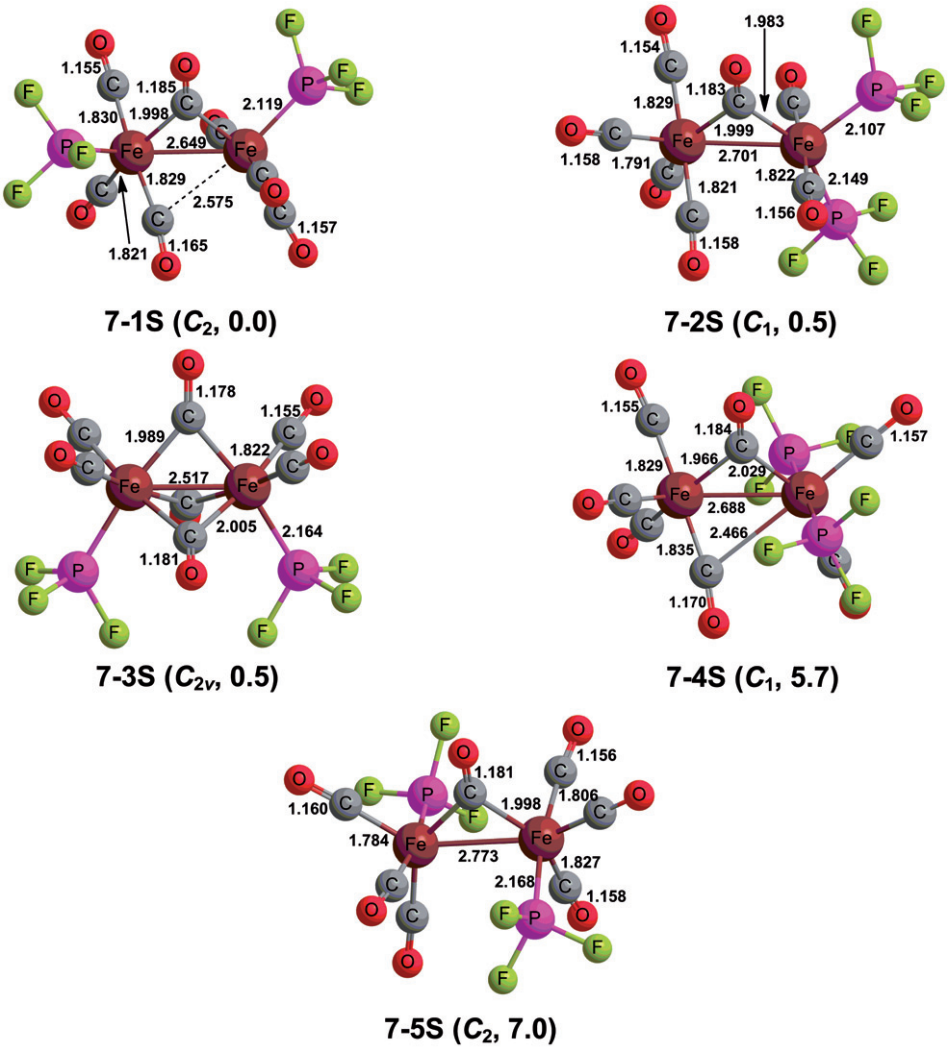

Figure 1. Optimized singlet $Fe_2(CO)_7(PF_3)_2$ structures and their relative energies (ΔE, in kcal mol^{-1}) using the B3LYP* method.

These spectroscopic data suggest that PF_3 is a slightly weaker backbonding ligand than CO.

3.2. *$Fe_2(CO)_6(PF_3)_2$*

Three triplet structures (**6-1T** to **6-3T** in figure 2 and table S2) and four singlet structures (**6-1S** to **6-4S** in figure 3 and table S2) are obtained for $Fe_2(CO)_6(PF_3)_2$. The global minimum predicted by the B3LYP* method is the triplet structure **6-1T**.

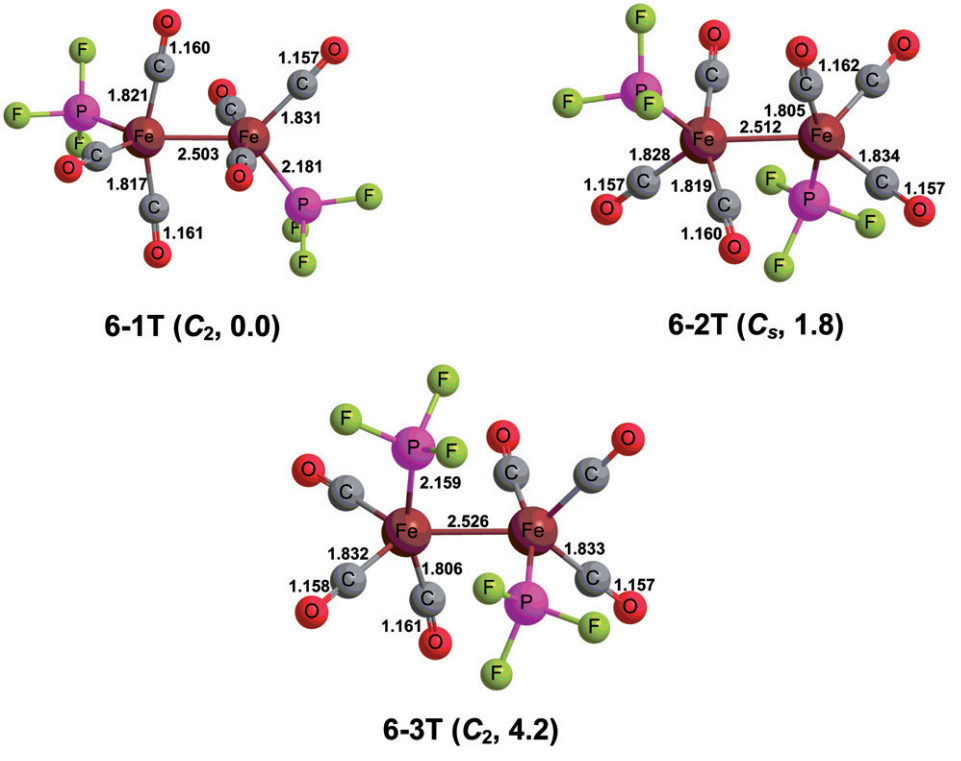

Figure 2. Optimized triplet $Fe_2(CO)_6(PF_3)_2$ structures and their relative energies (ΔE, in kcal mol^{-1}) using the B3LYP* method.

The lowest-lying $Fe_2(CO)_6(PF_3)_2$ structure is the C_2 triplet structure **6-1T** having all terminal ligands (figure 2 and table S2). The other two geometrically similar triplet $Fe_2(CO)_6(PF_3)_2$ structures **6-2T** (C_s) and **6-3T** (C_2) lie 1.8 and 4.2 kcal mol^{-1}, respectively, in energy above **6-1T**. The $Fe_2(CO)_6(PF_3)_2$ structures **6-2T** and **6-3T** differ from **6-1T** only in the locations of the terminal PF_3 groups. Structures **6-1T** and **6-3T** have all real vibrational frequencies. However, structure **6-2T** has a very small imaginary vibrational frequency of 12*i* cm^{-1}, which is removed using a finer (120, 974) integration grid. Thus all three triplet $Fe_2(CO)_6(PF_3)_2$ structures are genuine minima. The Fe=Fe bond distances for the three triplet structures fall in the range 2.50–2.53 Å, which is ~0.2 Å less than the Fe–Fe singly bridged single bond distances in the $Fe_2(CO)_7(PF_3)_2$ structures and thus can be interpreted as formal double bonds. This gives each iron in the triplet structures the favored 18-electron configuration. The triplet spin multiplicities in these $Fe_2(CO)_6(PF_3)_2$ structures arise from the Fe=Fe double bond, which is of the $\sigma + 2/2\pi$ type with unpaired electrons in each of the two orthogonal π compounds of the Fe=Fe bond. This type of Fe=Fe double bond containing two unpaired electrons is analogous to the O=O double bond in triplet dioxygen as well as the Fe=Fe double bond in the experimentally known [56, 57] $(\eta^5\text{–}C_5H_5)_2Fe_2(\mu\text{-}CO)_3$.

The four singlet $Fe_2(CO)_6(PF_3)_2$ structures **6-1S** (C_1), **6-2S** (C_2), **6-3S** (C_2), and **6-4S** (C_1) are all doubly bridged structures (figure 3 and table S2) differing only in the

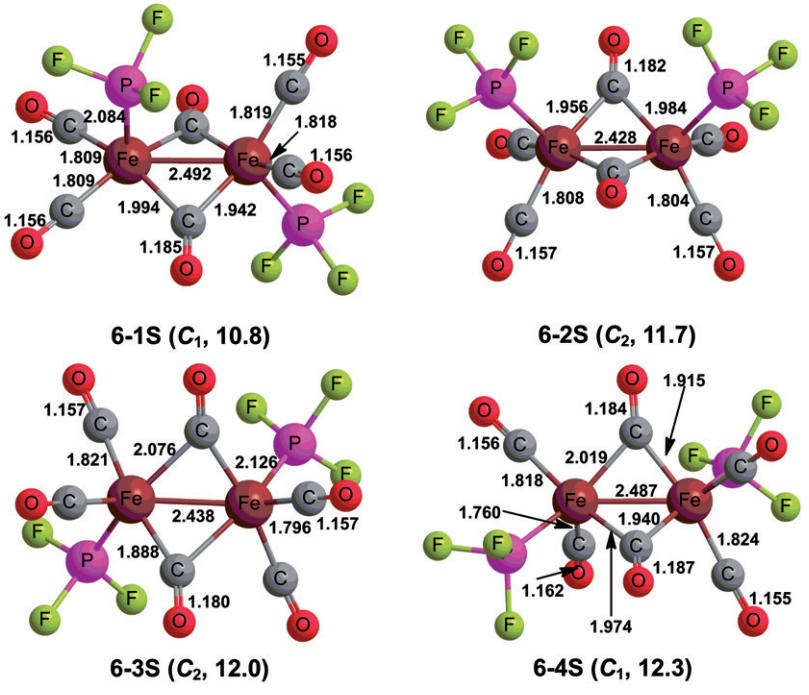

Figure 3. Optimized singlet $Fe_2(CO)_6(PF_3)_2$ structures and their relative energies (ΔE, in kcal mol^{-1}) using the B3LYP* method.

positions of the PF_3 and CO ligands. Their energies are close to each other within 1.5 kcal mol^{-1}, but approximately 10 kcal mol^{-1} above that of the triplet **6-1T** (table S2). The Fe=Fe bond distances in the four singlet structures ranging from 2.43 to 2.49 Å can correspond to formal double bonds, thereby giving each iron atom the favored 18-electron configuration.

3.3. *$Fe_2(CO)_5(PF_3)_2$*

Singlet, triplet, and quintet $Fe_2(CO)_5(PF_3)_2$ structures have been optimized. The B3LYP and BP86 methods predict different global minima. Thus the B3LYP method predicts a triplet structure for the global minimum, while the BP86 method predicts a singlet for the global minimum. This is another example of the tendency of the B3LYP method to favor higher spin states relative to the BP86 method [47, 48]. The B3LYP* method, which is more reliable for singlet–triplet splittings, predicts the triplet structure **5-1T** to be the global minimum.

The $Fe_2(CO)_5(PF_3)_2$ structures **5-1T**, **5-2T**, and **5-5T** are similar with a single semibridging carbonyl group (figure 4 and table S3). Their Fe=Fe distances of ~2.5 Å correspond to formal double bonds giving each iron a 17-electron configuration consistent with binuclear triplets. These three structures differ only in the locations of the PF_3 groups. Structure **5-1T** is the $Fe_2(CO)_5(PF_3)_2$ global minimum by the B3LYP* method. However, structure **5-2T** lies only 0.1 kcal mol^{-1} above **5-1T** so that these two

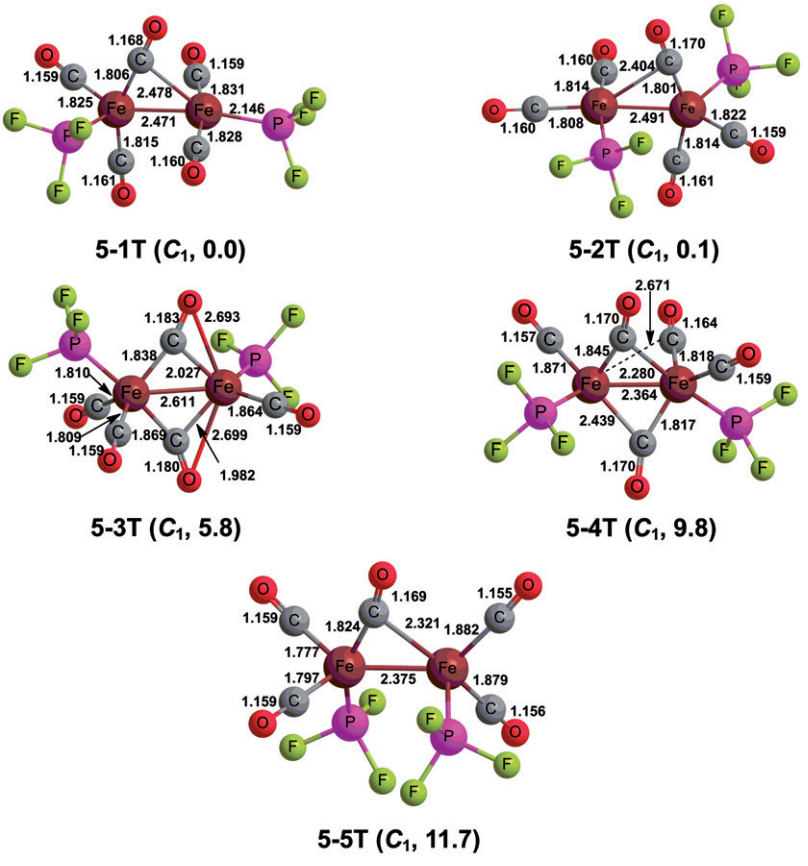

Figure 4. Optimized triplet $Fe_2(CO)_6(PF_3)_2$ structures and their relative energies (ΔE, in kcal mol^{-1}) using the B3LYP* method.

structures can be considered to be essentially degenerate. Structure **5-5T** lies at the significantly higher energy of 11.7 kcal mol^{-1} above **5-1T**. Structure **5-3T** lies 5.8 kcal mol^{-1} above **5-1T** and has two four-electron donor bridging CO groups, as indicated by Fe–O distances of ~2.7 Å. Structure **5-4T** (C_1) with two semibridging CO groups lies 9.8 kcal mol^{-1} above **5-1T**. Its Fe=Fe distance (~2.36 Å) suggests a formal double bond, thereby giving each iron a 17-electron configuration for a binuclear triplet.

The lowest lying of the singlet $Fe_2(CO)_5(PF_3)_2$ structures, **5-1S**, lies 3.9 kcal mol^{-1} above the global minimum **5-1T** (figure 5 and table S3). Structure **5-1S** has one normal two-electron donor bridging CO and one four-electron donor CO. The latter is indicated by the short Fe–O distance of 2.576 Å. The Fe–Fe distance of 2.422 Å in **5-1S** corresponds to a formal double bond. This gives each Fe the favored 18-electron configuration in this singlet $Fe_2(CO)_5(PF_3)_2$ with a single four-electron donor bridging CO group.

The remaining singlet $Fe_2(CO)_5(PF_3)_2$ structures have only two-electron donor CO groups and Fe≡Fe distances ranging from 2.15 to 2.20 Å suggesting the formal triple bonds required to give each iron the favored 18-electron configuration. Structure **5-2S**

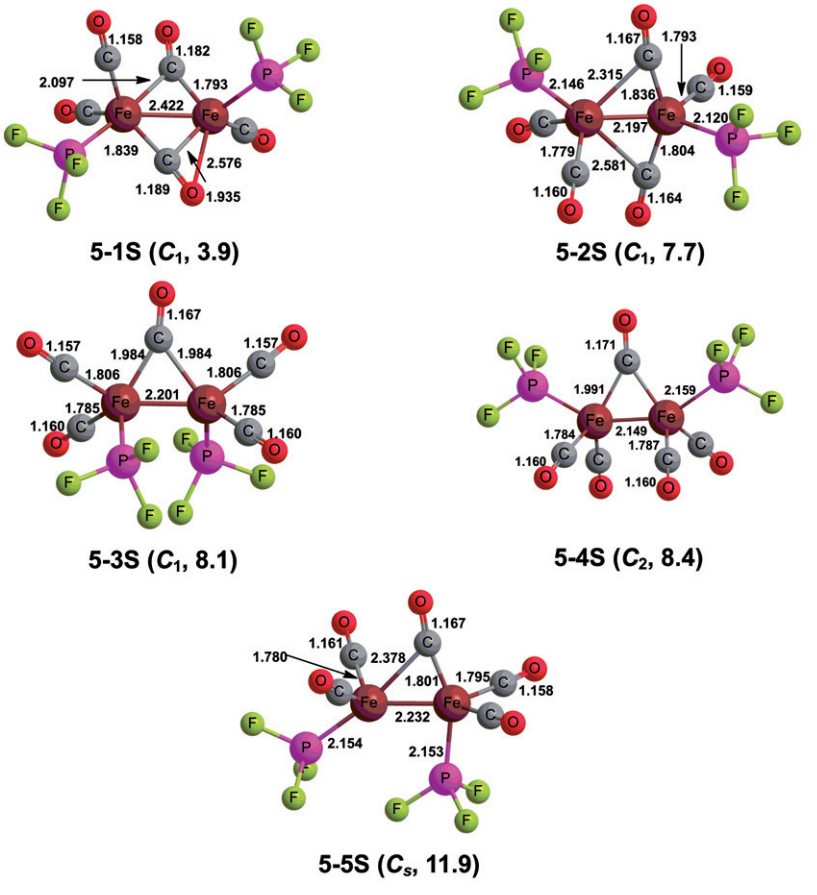

Figure 5. Optimized singlet $Fe_2(CO)_5(PF_3)_2$ structures and their relative energies (ΔE, in kcal mol^{-1}) using the B3LYP* method.

with two semibridging CO groups lies 7.7 kcal mol^{-1} above **5-1T**. The singly bridged structures **5-3S** and **5-4S** differ only in the locations of the two terminal PF_3 ligands. Structures **5-3S** and **5-4S** have similar energies of 8.1 and 8.4 kcal mol^{-1}, respectively, above **5-1T**. The other remaining singlet $Fe_2(CO)_5(PF_3)_2$ structure **5-5S**, lying 11.9 kcal mol^{-1} above **5-1T**, has a semibridging carbonyl.

Higher spin states of the highly unsaturated $Fe_2(CO)_5(PF_3)_2$ were also optimized. Three low-lying quintet structures with similar energies were found, each lying ~15 kcal mol^{-1} above the **5-1T** global minimum (figure 6 and table S3). Structures **5-1Q** and **5-2Q** have one bridging CO, whereas structure **5-3Q** has one normal bridging CO and one semibridging CO. The Fe–Fe distances in these quintet structures range from 2.52 to 2.54 Å suggesting formal single bonds giving each Fe a 16-electron configuration in these binuclear quintets.

3.4. *$Fe_2(CO)_4(PF_3)_2$*

Ten $Fe_2(CO)_4(PF_3)_2$ structures were optimized within ~20 kcal mol^{-1} of the global minimum (figures 7–9 and table S4). Three doubly CO-bridged triplet structures **4-1T**,

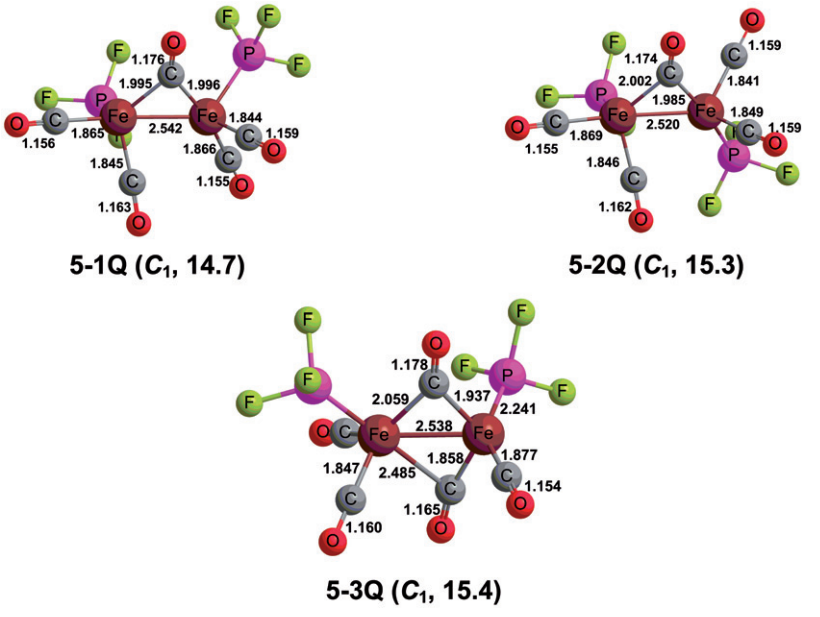

Figure 6. Optimized quintet $Fe_2(CO)_5(PF_3)_2$ structures and their relative energies (ΔE, in kcal mol^{-1}) using the B3LYP* method.

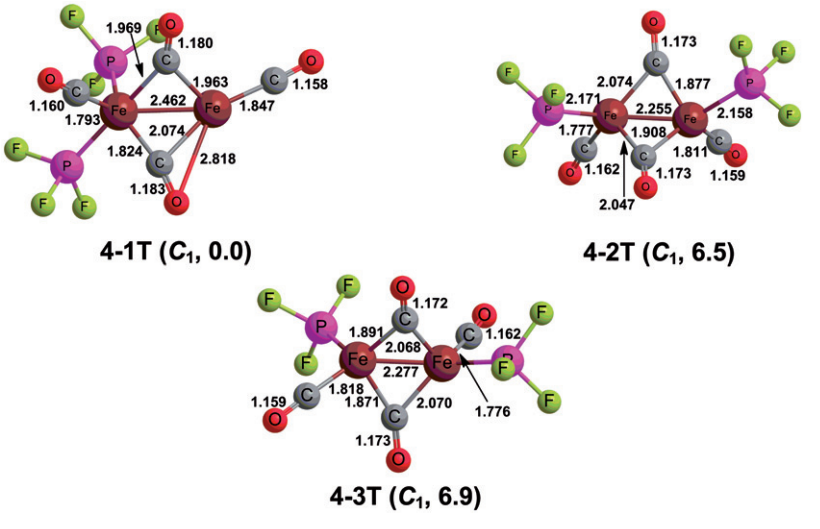

Figure 7. Optimized triplet $Fe_2(CO)_4(PF_3)_2$ structures and their relative energies (ΔE, in kcal mol^{-1}) using the B3LYP* method.

4-2T, and **4-3T** have the lowest energies (figure 7). Structure **4-1T** has one two-electron donor bridging CO and one four-electron bridging CO. The Fe=Fe distance of 2.462 Å in **4-1T** suggests a formal double bond, thereby giving each Fe a 17-electron configuration, if the Fe–Fe bond is polarized, corresponding to a binuclear triplet.

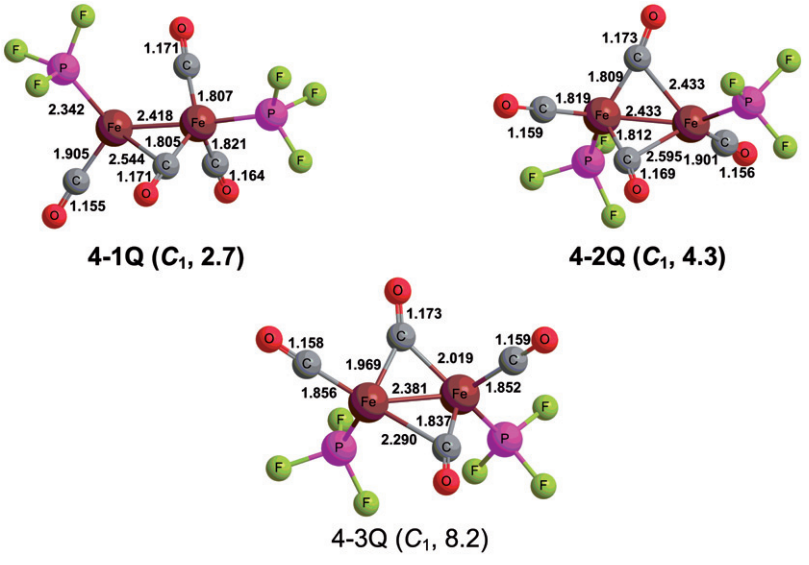

Figure 8. Optimized triplet $Fe_2(CO)_4(PF_3)_2$ structures and their relative energies (ΔE, in kcal mol^{-1}) using the B3LYP* method.

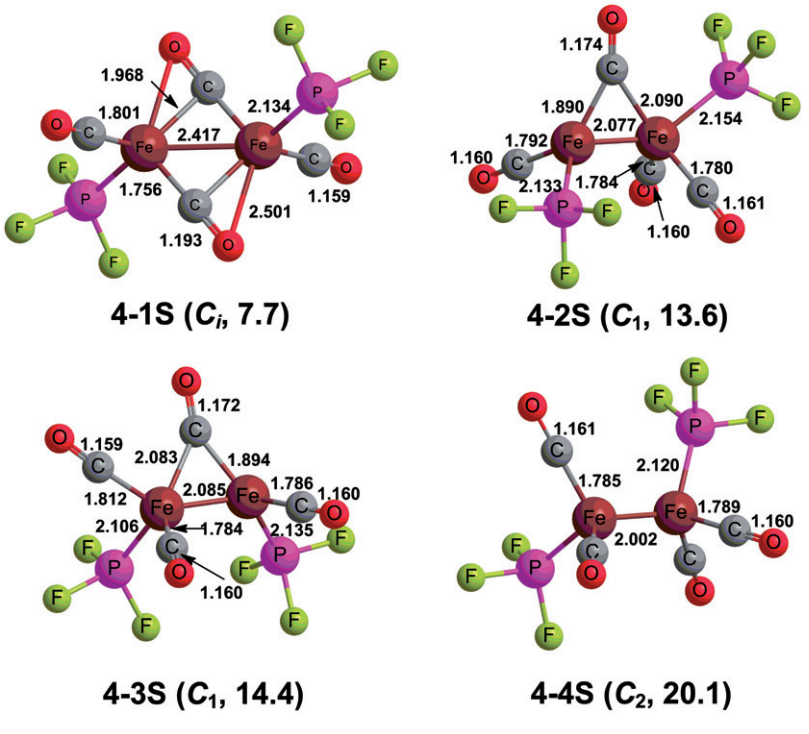

Figure 9. Optimized singlet $Fe_2(CO)_4(PF_3)_2$ structures and their relative energies (ΔE, in kcal mol^{-1}) using the B3LYP* method.

Structures **4-2T** and **4-3T** each have two two-electron donor bridging carbonyls. The Fe≡Fe distances in structures **4-2T** and **4-3T** of 2.26 to 2.28 Å suggest the formal triple bonds required to give each iron a 17-electron configuration consistent with a binuclear triplet.

The three quintet $Fe_2(CO)_4(PF_3)_2$ structures **4-1Q** (C_1), **4-2Q** (C_1), and **4-3Q** (C_1) lie ~3 to 8 kcal mol^{-1} in energy above **4-1T** (figure 8). Structures **4-1Q** and **4-2Q** each have a semibridging CO. Structure **4-2Q** has similar geometry with different relative position of the ligands. Structure **4-3Q** has two semibridging CO groups. The Fe=Fe distances ranging from 2.38 to 2.43 Å for the three quintet structures correspond to formal double bonds required to give each Fe a 16-electron configuration leading to a quintet spin state for a high-spin binuclear structure.

The singlet $Fe_2(CO)_4(PF_3)_2$ structures have somewhat higher energies (figure 9 and table S4). The C_i structure **4-1S** lies 7.7 kcal mol^{-1} above **4-1T**. Structure **4-1S** has two four-electron donor bridging COs. The Fe=Fe distance in **4-1S** of ~2.42 Å suggests a formal Fe–Fe double bond to give Fe the favored 18-electron configuration in a $Fe_2(CO)_4(PF_3)_2$ structure having two four-electron donor bridging CO groups.

The remaining $Fe_2(CO)_4(PF_3)_2$ structures all have very short Fe–Fe bonds of 2.0 to 2.1 Å. This can correspond to the formal quadruple bond required to give each iron the favored 18-electron configuration. The singly bridged structures **4-2S** and **4-3S** lie 13.6 and 14.4 kcal mol^{-1}, respectively, above **4-1T**. The unbridged $Fe_2(CO)_4(PF_3)_2$ structure **4-4S** is an even higher energy structure, lying 20.1 kcal mol^{-1} above the global minimum **4-1T.** The Fe–Fe distance of 2.002 Å in **4-4S** is the shortest iron–iron distance found in this work.

3.5. *Dissociation energies*

Table 1 reports the carbonyl dissociation energies (ΔE) of the lowest energy $Fe_2(CO)_n(PF_3)_2$ structures corresponding to the following type of reactions:

$$Fe_2(CO)_n(PF_3)_2 \rightarrow Fe_2(CO)_{n-1}(PF_3)_2 + CO \ (n = 7, 6, 5).$$

The energy (ΔE) required to remove one CO from the lowest energy binuclear structures of $Fe_2(CO)_n(PF_3)_2$ ($n = 7, 6, 5$) are 21.1 kcal mol^{-1} ($n = 7$), 34.5 kcal mol^{-1} ($n = 6$), and 34.2 kcal mol^{-1} ($n = 5$), respectively. These carbonyl dissociation energies are in the typical range for metal carbonyl derivatives, comparable to the corresponding experimental dissociation energies for $Ni(CO)_4$, $Fe(CO)_5$, and $Cr(CO)_6$ of 27 kcal mol^{-1}, 41 kcal mol^{-1}, and 37 kcal mol^{-1}, respectively [58]. These substantial ΔE values show that the $Fe_2(PF_3)_2(CO)_n$ ($n = 7, 6, 5$) complexes are all stable thermodynamically with respect to CO loss.

The disproportionation energies listed in table 1 correspond to reactions of the following type:

$$2Fe_2(CO)_n(PF_3)_2 \rightarrow Fe_2(CO)_{n+1}(PF_3)_2 + Fe_2(CO)_{n-1}(PF_3)_2 \ (n = 6, 5),$$

which are equal to the value of $\Delta E[Fe_2(PF_3)_2(CO)_n] - \Delta E[Fe_2(PF_3)_2(CO)_{n+1}]$. These values indicate that $Fe_2(CO)_6(PF_3)_2$ is favorable with respect to such disproportionation since it is predicted to require 13.7 kcal mol^{-1} to disproportionate into $Fe_2(CO)_7(PF_3)_2 + Fe_2(CO)_5(PF_3)_2$. However, the dissociation of $Fe_2(CO)_5(PF_3)_2$ into $Fe_2(CO)_6$

Table 1. Dissociation energies and disproportionation energies for the global minima of $Fe_2(PF_3)_2(CO)_n$ ($n = 7, 6, 5, 4$) using the B3LYP* method.

	B3LYP*
$Fe_2(CO)_7(PF_3)_2 \rightarrow Fe_2(CO)_6(PF_3)_2 + CO$	21.1
$Fe_2(CO)_6(PF_3)_2 \rightarrow Fe_2(CO)_5(PF_3)_2 + CO$	34.5
$Fe_2(CO)_5(PF_3)_2 \rightarrow Fe_2(CO)_4(PF_3)_2 + CO$	34.2
$2\ Fe_2(CO)_6(PF_3)_2 \rightarrow Fe_2(CO)_7(PF_3)_2 + Fe_2(CO)_5(PF_3)_2$	13.4
$2\ Fe_2(CO)_5(PF_3)_2 \rightarrow Fe_2(CO)_6(PF_3)_2 + Fe_2(CO)_4(PF_3)_2$	−0.3
$Fe_2(CO)_7(PF_3)_2 \rightarrow Fe(CO)_5 + Fe(CO)_2(PF_3)_2$	29.3
$Fe_2(CO)_7(PF_3)_2 \rightarrow Fe(CO)_4 + Fe(CO)_3(PF_3)_2$	17.4
$Fe_2(CO)_7(PF_3)_2 \rightarrow Fe(CO)_4(PF_3) + Fe(CO)_3(PF_3)$	20.0
$Fe_2(CO)_6(PF_3)_2 \rightarrow 2\ Fe(CO)_3(PF_3)$	46.5
$Fe_2(CO)_6(PF_3)_2 \rightarrow Fe(CO)_4(PF_3) + Fe(CO)_2(PF_3)$	47.9
$Fe_2(CO)_6(PF_3)_2 \rightarrow Fe(CO)_3(PF_3)_2 + Fe(CO)_3$	51.9
$Fe_2(CO)_6(PF_3)_2 \rightarrow Fe(CO)_4 + Fe\ (CO)_2(PF_3)_2$	46.1
$Fe_2(CO)_5(PF_3)_2 \rightarrow Fe(CO)_4 + Fe(CO)(PF_3)_2$	63.3
$Fe_2(CO)_5(PF_3)_2 \rightarrow Fe(CO)_3(PF_3) + Fe(CO)_2(PF_3)$	61.0
$Fe_2(CO)_5(PF_3)_2 \rightarrow Fe_2(CO)_3 + Fe_2(CO)_2(PF_3)_2$	67.2
$Fe_2(CO)_4(PF_3)_2 \rightarrow Fe(CO)_3 + Fe(CO)(PF_3)_2$	84.6
$Fe_2(CO)_4(PF_3)_2 \rightarrow 2\ Fe(CO)_2(PF_3)$	75.8

$(PF_3)_2 + Fe_2(CO)_4(PF_3)_2$ is essentially thermoneutral suggesting that $Fe_2(CO)_5(PF_3)_2$ is not a viable species.

Table 1 also reports the energies for the dissociation of binuclear $Fe_2(PF_3)_2(CO)_n$ into mononuclear fragments by reactions of the general type:

$$Fe_2(CO)_n(PF_3)_2 \rightarrow Fe_2(CO)_x(PF_3)_a + Fe(CO)_y(PF_3)_b\ (n = 7, 6, 5, 4, x + y = n, a + b = 2).$$

All such dissociations are highly endothermic by at least 45 kcal mol^{-1}, except for those for $Fe_2(CO)_7(PF_3)_2$, which fall in the range 17–30 kcal mol^{-1} depending on the mononuclear fragments produced. The lowest energy dissociation process for $Fe_2(CO)_7(PF_3)_2$ is the dissociation into $Fe(CO)_4 + Fe(CO)_3(PF_3)_2$, which is predicted to require 17.4 kcal mol^{-1}. These dissociation energy values confirm that all of the binuclear $Fe_2(CO)_n(PF_3)_2$ structures are stable relative to dissociation into mononuclear complexes.

3.6. *Atomic population, natural bonding orbital analysis, and iron–iron bonding*

Table 2 lists the natural charges for the two Fe atoms, the Wiberg bond indices (WBIs) for the iron–iron bonds, and the Fe–Fe distances for the singlet $Fe_2(PF_3)_2(CO)_n$ complexes obtained by natural bonding orbital (NBO) [59] analysis using Gaussian03 (C.02) program [54].

The WBI values for the Fe–Fe single bonds in $Fe_2(CO)_7(PF_3)_2$ structures fall in the narrow range of 0.11–0.12. The WBI values for the Fe=Fe double bonds in the singlet $Fe_2(CO)_6(PF_3)_2$ structures are consistently higher in the range 0.27–0.36. For the more highly unsaturated $Fe_2(CO)_n(PF_3)_2$ structures with formal Fe=Fe double bonds and containing four-electron donor bridging CO groups, the WBIs are consistently higher. Thus the Fe=Fe double bond in $Fe_2(CO)_5(PF_3)_2$ structure **5-1S** with one four-electron donor bridging CO group has a WBI of 0.36. The Fe≡Fe triple bonds in

Table 2. Atomic population, NBO analysis, and iron–iron bonding by the B3LYP* method.

Structures	Natural charge on Fe/Fe	WBI	Fe–Fe distance (Å)	Formal Fe–Fe bond order
7-1S	−0.68/−0.68	0.12	2.649	1
7-2S	−0.51/−0.82	0.12	2.701	1
7-3S	−0.71/−0.71	0.11	2.517	1
7-4S	−0.54/−0.78	0.11	2.688	1
7-5S	−0.61/−0.61	0.11	2.773	1
6-1S	−0.44/−0.58	0.29	2.492	2
6-2S	−0.52/−0.52	0.36	2.428	2
6-3S	−0.52/−0.52	0.35	2.438	2
6-4S	−0.40/−0.56	0.27	2.487	2
5-1S	−0.53/−0.25	0.36	2.422	2
5-2S	−0.31/−0.55	0.54	2.197	3
5-3S	−0.46/−0.46	0.54	2.201	3
5-4S	−0.39/−0.39	0.63	2.149	3
5-5S	−0.34/−0.53	0.52	2.232	3
4-1S	−0.26/−0.26	0.49	2.417	2
4-2S	−0.30/−0.34	0.91	2.077	4
4-3S	−0.37/−0.34	0.89	2.085	4
4-4S	−0.40/−0.40	0.86	2.002	4

$Fe_2(CO)_5(PF_3)_2$ have even higher WBIs from 0.52–0.64. As expected the highest WBIs of ~0.9 are found for the formal Fe–Fe quadruple bonds in $Fe_2(CO)_4(PF_3)_2$ structures.

The natural atomic charges on Fe are related to the number of CO and PF_3 ligands connected directly to Fe with an increasing number of such ligands leading to an increased negative charge (table 2). Thus the backbonding of the Fe d electrons into the antibonding orbitals of CO and PF_3, although strong relative to most other ligands, is not sufficient to remove all of the negative charge resulting from the forward σ-bonding of such ligands to Fe. However, since backbonding capabilities of CO and PF_3, although strong, are not the same, the relationship between the iron natural atomic charge and the number of ligands is not a simple relationship.

4. Discussion

The low-energy $Fe_2(CO)_n(PF_3)_2$ ($n = 7, 6, 5, 4$) structures found in this work have the following general features: (1) the complete absence of bridging PF_3 groups whereas most of the structures have bridging CO groups; and (2) the preference for structures with a symmetrical distribution of the PF_3 ligands with each iron atom bearing a single PF_3 over structures with an unsymmetrical distribution of PF_3 ligands with one iron bearing two PF_3 and the other iron bearing none. Thus, the only structures in which one iron is bonded to both PF_3 ligands and the other iron to no PF_3 ligands are $Fe_2(CO)_6(PF_3)_2$ structures **7-2S** and **7-4S** (figure 1).

The absence of bridging PF_3 groups in structures having bridging carbonyl groups can be rationalized by comparing the coordination numbers of the donors in the terminal and bridging structures (figure 10). For a terminal CO group the carbon is two-coordinate with linear sp hybridization. When a CO group bridges a pair of metal

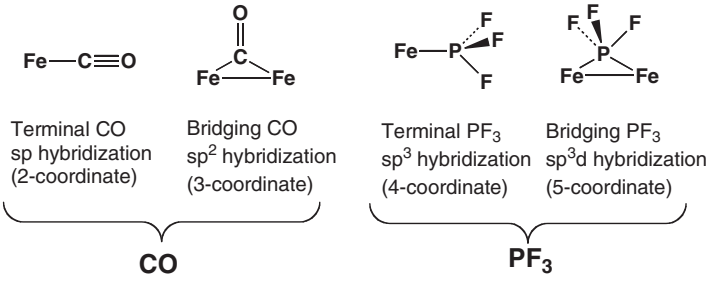

Figure 10. A comparison of the donor atom environments for terminal and bridging CO and PF_3 groups.

atoms the carbon coordination number increases to three corresponding to distorted trigonal sp^2 hybridization. This increase in coordination number poses no difficulty and is analogous to addition reactions to carbon–carbon triple bonds in alkynes to give alkene derivatives. For a terminal PF_3 group the phosphorus is four-coordinate with tetrahedral sp^3 hybridization. However, formation of a PF_3 bridge between two metals forces the phosphorus to become five-coordinate. Five-coordinate phosphorus is known in hypervalent species (e.g., PF_5) and traditionally (and mathematically) can be considered as involving dsp^3 hybridization but alternatively can involve a four-electron, three-center bond and thus use only the phosphorus sp^3 orbital manifold. In any case going from two-coordinate to three-coordinate carbon in converting a terminal CO group to a bridging CO group is a more favorable process than going from four-coordinate to five-coordinate phosphorus in converting a terminal PF_3 to a bridging PF_3.

The apparent reluctance of $Fe_2(CO)_n(PF_3)_2$ derivatives to form structures with two PF_3 groups bonded to the same iron can be related to the increased steric demands of a PF_3 ligand relative to a CO ligand (figure 10). Carbonyl groups are compact linear ligands with minimal steric requirements. However, the fluorines bonded to phosphorus in PF_3 make PF_3 more sterically demanding than CO. Thus in binuclear metal carbonyl trifluorophosphines containing only CO and PF_3, it is more energetically efficient to distribute the significantly larger PF_3 ligands evenly between metals.

It is instructive to compare the structures of the ternary iron carbonyl trifluorophosphine complexes $Fe_2(CO)_n(PF_3)_2$ with those of the corresponding binary iron carbonyls $Fe_2(CO)_{n+2}$. The only binary iron carbonyl that is known experimentally is $Fe_2(CO)_9$, which has a triply bridged structure as determined by X-ray crystallography [2, 3]. DFT using the BP86 method predicts this triply bridged $Fe_2(CO)_6(\mu\text{-}CO)_3$ structure to be the lowest energy structure [46, 60]. A singly bridged $Fe_2(CO)_8(\mu\text{-}CO)$ structure is also found for $Fe_2(CO)_9$ but at 3 to 6 kcal mol^{-1} above the triply bridged structure. For the ternary trifluorophosphine complex $Fe_2(CO)_7(PF_3)_2$ the singly bridged structure **7-2S** and the triply bridged structure **7-3S** have essentially the same energies (figure 1 and table S1). Also of comparable energy is the $Fe_2(CO)_7(PF_3)_2$ structure **7-1S** with a single symmetrical bridging CO group and a highly unsymmetrical semibridging CO group.

For the unsaturated $Fe_2(CO)_n(PF_3)_2$ ($n = 6, 5, 4$) derivatives the lowest energy structures by the B3LYP* method are triplet spin-state structures, not found in the work on the corresponding homoleptic $Fe_2(CO)_{n+2}$ derivatives [8]. The lowest energy

$Fe_2(CO)_6(PF_3)_2$ structures are unbridged triplet structures with Fe=Fe distances of ~2.5 Å interpreted as formal double bonds (figure 2). In these triplet spin-state structures, the two unpaired electrons lie in the two orthogonal π components of a $\sigma + 2/2\,\pi$ type Fe=Fe double bond, similar to the O=O double bond in triplet dioxygen and the Fe=Fe double bond in $(\eta^5\text{-}Me_5C_5)_2Fe_2(\mu\text{-}CO)_3$ [56, 57]. The lowest energy singlet $Fe_2(CO)_6(PF_3)_2$ structures have two bridging CO groups and Fe=Fe distances of 2.4 to 2.5 Å corresponding to the formal double bonds required to give iron the favored 18-electron configuration. The lowest energy $Fe_2(CO)_8$ structures are similar doubly bridged structures [8].

The 18-electron rule predicts a formal Fe≡Fe triple bond in singlet $Fe_2(CO)_5(PF_3)_2$ or $Fe_2(CO)_7$ structures containing only two-electron donor CO groups. However, the lowest energy singlet $Fe_2(CO)_5(PF_3)_2$ structure **5-1S** (figure 5) has a four-electron donor bridging CO group with a short Fe–O distance of 2.576 Å and an Fe=Fe distance of 2.422 Å suggesting the formal double bond required to give both irons the favorable 18-electron configuration. A related structure with a similar four-electron donor bridging CO group and an Fe=Fe distance suggesting a formal double bond was not found for $Fe_2(CO)_7$ [8]. Several higher energy singlet $Fe_2(CO)_5(PF_3)_2$ structures were found with all two-electron donor carbonyl groups and Fe≡Fe distances of ~2.2 Å suggesting formal triple bonds. The $Fe_2(CO)_5(PF_3)_2$ structure **5-2S** (figure 5) with two semibridging CO groups is analogous to the lowest energy $Fe_2(CO)_7$ structure. However, **5-2S** lies 3.8 kcal mol^{-1} above the lowest energy singlet $Fe_2(CO)_5(PF_3)_2$ structure **5-1S** and 7.7 kcal mol^{-1} above the triplet global minimum **5-1T**.

The 18-electron rule predicts a formal Fe–Fe quadruple bond for $Fe_2(CO)_4(PF_3)_2$ and $Fe_2(CO)_6$ if all of the carbonyl groups are two-electron donors. However, the lowest energy singlet $Fe_2(CO)_4(PF_3)_2$ structure **4-1S** (figure 9) has two four-electron donor bridging CO groups and a Fe=Fe distance of ~2.42 Å corresponding to the formal double bond required to give both irons the favored 18-electron configuration. However, three higher energy singlet $Fe_2(CO)_4(PF_3)_2$ structures were found with all two-electron donor CO groups and ultrashort Fe–Fe distances of 2.0 to 2.1 Å suggesting formal quadruple bonds (figure 9). These singlet $Fe_2(CO)_4(PF_3)_2$ structures are analogous to the previously studied $Fe_2(CO)_6$ structures [8]. Thus the lowest energy $Fe_2(CO)_6$ structure has two four-electron donor CO groups and a ~2.43 Å Fe=Fe double bond distance. Higher energy $Fe_2(CO)_6$ structures are found with all two-electron donor CO groups and ultrashort Fe–Fe distances of ~2.0 Å suggesting formal quadruple bonds.

5. Summary

None of the low-energy $Fe_2(CO)_n(PF_3)_2$ ($n = 7, 6, 5, 4$) structures optimized by DFT have bridging PF_3 groups even though many such structures have one or more bridging CO groups. Thus bridging PF_3 groups are clearly very unfavorable relative to terminal PF_3 groups. All except for some of the $Fe_2(CO)_7(PF_3)_2$ structures have each PF_3 bonded to a different iron. The lowest energy structures for the unsaturated $Fe_2(CO)_n(PF_3)_2$ ($n = 6, 5, 4$) derivatives are triplet spin-state structures. However, higher energy singlet $Fe_2(CO)_n(PF_3)_2$ ($n = 6, 5, 4$) structures are found with formal iron–iron multiple bonds and various combinations of bridging and terminal CO

groups leading to the favored 18-electron configurations for iron. Most of these structures are analogous to previously studied $Fe_2(CO)_{n+2}$ structures. These highly unsaturated singlet structures include singlet $Fe_2(CO)_4(PF_3)_2$ structures with ultrashort Fe–Fe distances of ~2.0 Å suggesting the formal quadruple bonds required to give each iron the favored 18-electron configuration.

Supplementary material

Tables S1–S4: Total energies (E, in Hartree), relative energies (ΔE, in kcal mol^{-1}), relative energies corrected by ZPE (ΔE_{ZPE}, in kcal mol^{-1}), numbers of imaginary vibrational frequencies (Nimg), and spin contamination ($\langle S^2 \rangle$) for the optimized structures of $Fe_2(CO)_n(PF_3)_2$ ($n = 7, 6, 5, 4$) by the B3LYP* method; figures S1–S9: optimized structures by B3LYP (top), BP86 (middle), and B3LYP* (bottom) methods; tables S5–S13: total energies (E, in Hartree), relative energies (ΔE, in kcal mol^{-1}), relative energies corrected by ZPE (ΔE_{ZPE}, in kcal mol^{-1}), numbers of imaginary vibrational frequencies (Nimg), and spin contamination ($\langle S^2 \rangle$) for the optimized structures of $Fe_2(CO)_n(PF_3)_2$ ($n = 7, 6, 5, 4$) by the B3LYP and BP86 methods; table S14: dissociation energies and disproportionation energies of $Fe_2(PF_3)_2(CO)_n$ ($n = 7, 6, 5, 4$) by the B3LYP and BP86 methods; tables S15–S16: atomic population, NBO analysis, and iron–iron bonding by the B3LYP and BP86 methods; tables S17–S20: harmonic vibrational frequencies (cm^{-1}) and corresponding infrared intensities (in parentheses) predicted by the BP86 method for the optimized structures $Fe_2(CO)_7(PF_3)_2$, $Fe_2(CO)_6(PF_3)_2$, $Fe_2(CO)_7(PF_3)_2$, and $Fe_2(CO)_7(PF_3)_2$; tables S21–S24: the ν(CO) stretching frequencies predicted for the binuclear $Fe_2(CO)_7(PF_3)_2$, $Fe_2(CO)_6(PF_3)_2$, $Fe_2(CO)_7(PF_3)_2$, and $Fe_2(CO)_7(PF_3)_2$ by the BP86 method; tables S25–S28: the $\nu(PF_3)$ stretching frequencies predicted for the binuclear $Fe_2(CO)_7(PF_3)_2$, $Fe_2(CO)_6(PF_3)_2$, $Fe_2(CO)_7(PF_3)_2$, and $Fe_2(CO)_7(PF_3)_2$ by the BP86 method; tables S29–S32: cartesian coordinates for the optimized structures $Fe_2(CO)_7(PF_3)_2$, $Fe_2(CO)_6(PF_3)_2$, $Fe_2(CO)_7(PF_3)_2$, and $Fe_2(CO)_7(PF_3)_2$ by the B3LYP, BP86, and B3LYP* methods; complete Gaussian 03 reference (Ref. [54]).

Acknowledgments

We are indebted to the U.S. National Science Foundation (Grant CHE-1057466), the National Natural Science Foundation of China (20973066), the Doctoral Program of Higher Education (20104407110007) of China, and the Guangdong Provincial Natural Science Foundation of China (Grant S2011010003399) for support of this research.

References

[1] J. Dewar, F.R.S. Jackson, H.O. Jones. *Proc. R. Soc. (London) A*, **76**, 558 (1905).
[2] H.M. Powell, R.V.G. Ewens. *J. Chem. Soc.*, 286 (1939).
[3] F.A. Cotton, J.M. Troup. *J. Chem. Soc., Dalton Trans.*, 800 (1974).
[4] M. Poliakoff, J.J. Turner. *J. Chem. Soc. A*, 2403 (1971).

[5] S.C. Fletcher, M. Poliakoff, J.J. Turner. *Inorg. Chem.*, **25**, 3597 (1986).
[6] S. Fedrigo, T.L. Haslett, M. Moskovits. *J. Am. Chem. Soc.*, **118**, 5083 (1996).
[7] J.H. Jang, J.G. Lee, H. Lee, Y. Xie, H.F. Schaefer. *J. Phys. Chem. A*, **102**, 5298 (1998).
[8] Y. Xie, H.F. Schaefer, R.B. King. *J. Am. Chem. Soc.*, **122**, 8746 (2000).
[9] J.C. Green, D.I. King, J.H.D. Eland. *J. Chem. Soc. D*, 1121 (1970).
[10] I.H. Hiller, V.R. Saunders, M.J. Ware, P.J. Bassett, D.R. Lloyd, N. Lynaugh. *J. Chem. Soc. D*, 1316 (1970).
[11] P.J. Bassett, B.R. Higginson, D.R. Lloyd, N. Lynaugh, P.J. Roberts. *J. Chem. Soc., Dalton Trans.*, 2316 (1974).
[12] J. Müller, K. Fenderl, B. Mertschenk. *Chem. Ber.*, **104**, 700 (1971).
[13] R.A. Head, J.F. Nixon, G.J. Sharp, R.J. Clark. *J. Chem. Soc., Dalton Trans.*, 2054 (1975).
[14] J.F. Nixon, E.A. Seddon, R.J. Suffolk, M.J. Taylor, J.C. Green, R.J. Clark. *J. Chem. Soc., Dalton Trans.*, 765 (1986).
[15] J.-M. Savariault, A. Serafini, M. Pellissier, P. Cassoux. *Theor. Chem. Acc.*, **42**, 155 (1976).
[16] M. Braga. *Inorg. Chem.*, **24**, 2702 (1985).
[17] M. Braga. *J. Mol. Struct. Theochem.*, **253**, 167 (1992).
[18] G. Frenking, K. Wichmann, N. Fröhlich, J. Grobe, W. Golla, D. Le Van, B. Krebs, M. Läge. *Organometallics*, **21**, 2921 (2002).
[19] J.W. Irvine, G. Wilkinson. *Science*, **113**, 742 (1951).
[20] G. Wilkinson. *J. Am. Chem. Soc.*, **73**, 5501 (1951).
[21] T. Kruck. *Angew. Chem. Int. Ed.*, **6**, 53 (1967).
[22] T. Kruck. *Z. Naturforsch.*, **19**, 164 (1964).
[23] T. Kruck, K. Baur. *Angew. Chem.*, **77**, 505 (1965).
[24] T. Kruck, K. Baur. *Z. Anorg. Allg. Chem.*, **364**, 192 (1969).
[25] M.A. Bennett, R.N. Johnson, T.W. Turney. *Inorg. Chem.*, **15**, 2938 (1976).
[26] T. Drews, D. Rusch, S. Seidel, S. Willemsen, K. Seppelt. *Chem. Eur. J.*, **14**, 4280 (2008).
[27] P.L. Timms. *Chem. Commun.*, 1033 (1969).
[28] H.-q. Yang, Q.-s. Li, Y. Xie, R.B. King, H.F. Schaefer. *Mol. Phys.*, **108**, 2477 (2010).
[29] R. Zou, Q.-s. Li, Y. Xie, R.B. King, H.F. Schaefer. *Chem. Eur. J.*, **14**, 11149 (2008).
[30] T. Kruck, A. Prasch. *Angew. Chem.*, **76**, 892 (1964).
[31] T. Kruck, A. Prasch. *Z. Anorg. Allg. Chem.*, **356**, 118 (1968).
[32] R.J. Clark. *Inorg. Chem.*, **3**, 1395 (1964).
[33] T. Ziegler, J. Autschbach. *Chem. Rev.*, **105**, 2695 (2005).
[34] M. Bühl, H. Kabrede. *J. Chem. Theory Comput.*, **2**, 1282 (2006).
[35] M. Brynda, L. Gagliardi, P.O. Widmark, P.P. Power, B.O. Roos. *Angew. Chem. Int. Ed.*, **45**, 3804 (2006).
[36] N. Sieffert, M. Bühl. *J. Am. Chem. Soc.*, **132**, 8056 (2010).
[37] P. Schyman, W. Lai, H. Chen, Y. Wang, S. Shaik. *J. Am. Chem. Soc.*, **133**, 7977 (2011).
[38] R.D. Adams, W.C. Pearl, Y.O. Wong, Q. Zhang, M.B. Hall, J.R. Walensky. *J. Am. Chem. Soc.*, **133**, 12994 (2011).
[39] R. Lonsdale, J. Olah, A.J. Mulholland, J.A. Harvey. *J. Am. Chem. Soc.*, **133**, 15464 (2011).
[40] A.D. Becke. *J. Chem. Phys.*, **98**, 5648 (1993).
[41] C. Lee, W. Yang, R.G. Parr. *Phys. Rev. B*, **37**, 785 (1988).
[42] A.D. Becke. *Phys. Rev. A*, **18**, 3098 (1988).
[43] J.P. Perdew. *Phys. Rev. B*, **33**, 8822 (1986).
[44] F. Furche, J.P. Perdew. *J. Chem. Phys.*, **124**, 044103 (2006).
[45] H. Wang, Y. Xie, R.B. King, H.F. Schaefer. *J. Am. Chem. Soc.*, **127**, 11646 (2005).
[46] H. Wang, Y. Xie, R.B. King, H.F. Schaefer. *J. Am. Chem. Soc.*, **128**, 11376 (2006).
[47] M. Reiher, O. Salomon, B.A. Hess. *Theor. Chem. Acc.*, **107**, 48 (2001).
[48] O. Salomon, M. Reiher, B.A. Hess. *J. Chem. Phys.*, **117**, 4729 (2002).
[49] S. Huzinaga. *J. Chem. Phys.*, **42**, 1293 (1965).
[50] T.H. Dunning. *J. Chem. Phys.*, **53**, 2823 (1970).
[51] T.H. Dunning, P.J. Hay. In *Methods of Electronic Structure Theory*, H.F. Schaefer (Ed.), Vol. 3, pp. 1–27, Plenum, New York (1977).
[52] A.J.H. Wachters. *J. Chem. Phys.*, **52**, 1033 (1970).
[53] D.M. Hood, R.M. Pitzer, H.F. Schaefer. *J. Chem. Phys.*, **71**, 705 (1979).
[54] M.J. Frisch, G.W. Trucks, H.B. Schlegel, G.E. Scuseria, M.A. Robb, J.R. Cheeseman, Jr. J.A. Montgomery, T. Vreven, K.N. Kudin, J.C. Burant, J.M. Millam, S.S. Iyengar, J. Tomasi, V. Barone, B. Mennucci, M. Cossi, G. Scalmani, N. Rega, G.A. Petersson, H. Nakatsuji, M. Hada, M. Ehara, K. Toyota, R. Fukuda, J. Hasegawa, M. Ishida, T. Nakajima, Y. Honda, O. Kitao, H. Nakai, M. Klene, X. Li, J.E. Knox, H.P. Hratchian, J.B. Cross, V. Bakken, C. Adamo, J. Jaramillo, R. Gomperts, R.E. Stratmann, O. Yazyev, A.J. Austin, R. Cammi, C. Pomelli, J.W. Ochterski, P.Y. Ayala, K. Morokuma, G.A. Voth, P. Salvador, J.J. Dannenberg, V.G. Zakrzewski, S. Dapprich, A.D. Daniels, M.C. Strain, O. Farkas, D.K. Malick, A.D. Rabuck, K. Raghavachari, J.B. Foresman, J.V. Ortiz, Q. Cui, A.G. Baboul, S. Clifford, J. Cioslowski, B.B. Stefanov, G. Liu, A. Liashenko, P. Piskorz,

I. Komaromi, R.L. Martin, D.J. Fox, T. Keith, M.A. Al-Laham, C.Y. Peng, A. Nanayakkara, M. Challacombe, P.M.W. Gill, B. Johnson, W. Chen, M.W. Wong, C. Gonzalez, J.A. Pople. *Gaussian 03, Revisions E.01 and C.02*, Gaussian, Inc., Wallingford, CT (2004).
[55] J.M.L. Martin, C.W. Bauschlicher, A. Ricca. *Comput. Phys. Commun.*, **133**, 189 (2001).
[56] J.V. Caspar, T.J. Meyer. *J. Am. Chem. Soc.*, **102**, 7794 (1980).
[57] A.F. Hepp, J.P. Blaha, C. Lewis, M.S. Wrighton. *Organometallics*, **3**, 174 (1984).
[58] L.S. Sunderlin, D. Wang, R.R. Squires. *J. Am. Chem. Soc.*, **115**, 12060 (1993).
[59] A.E. Reed, L.A. Curtiss, F. Weinhold. *Chem. Rev.*, **88**, 899 (1988).
[60] E. Hunstock, C. Mealli, M.J. Calhorda, J. Reinhold. *Inorg. Chem.*, **38**, 5053 (1999).